ACS OMEGA

Article

Cite This: ACS Omega 2018, 3, 16338−16346

http://pubs.acs.org/journal/acsodf

Design and Synthesis of Imidazo/Benzimidazo[1,2-*c*]quinazoline Derivatives and Evaluation of Their Antimicrobial Activity

Nitesh Kumar Nandwana,[†] Rajnish Prakash Singh,[‡] Om P. S. Patel,[†] Shiv Dhiman,[†] Hitesh Kumar Saini,[†] Prabhat N. Jha,[‡] and Anil Kumar*[,†]

[†]Department of Chemistry and [‡]Department of Biological Sciences, Birla Institute of Technology and Science, Pilani 333031, Rajasthan, India

Supporting Information

ABSTRACT: A new class of fused quinazolines has been designed and synthesized via copper-catalyzed Ullmann type C−N coupling followed by intramolecular cross-dehydrogenative coupling reaction in moderate to good yields. The synthesized compounds were tested for in vitro antibacterial activity against three Gram negative (*Escherichia coli*, *Pseudomonas putida*, and *Salmonella typhi*) and two Gram positive (*Bacillus subtilis*, and *Staphylococcus aureus*) bacteria. Among all tested compounds, **8ga**, **8gc**, and **8gd** exhibited promising minimum inhibitory concentration (MIC) values (4−8 μg/mL) for all bacterial strains tested as compared to the positive control ciprofloxacin. The synthesized compounds were also evaluated for their in vitro antifungal activity against *Aspergillus niger* and *Candida albicans* and compounds **8ga**, **8gc**, and **8gd** having potential antibacterial activity also showed pronounced antifungal activity (MIC values 8−16 μg/mL) against both strains. The bactericidal assay by propidium iodide and live−dead bacterial cell screening using a mixture of acridine orange/ethidium bromide (AO/Et·Br) showed considerable changes in the bacterial cell membrane, which might be the cause or consequence of cell death. Moreover, the hemolytic activity for most potent compounds (**8ga**, **8gc**, and **8gd**) showed their safety profile toward human blood cells.

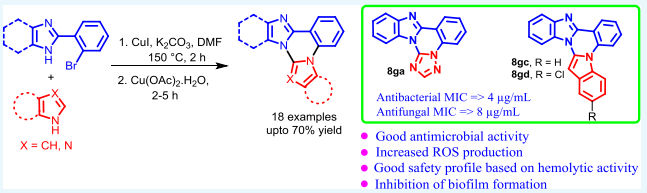

1. INTRODUCTION

Bacterial and fungal infections have become a global challenge for human health because of the lack of sufficient and effective antimicrobial drugs, especially in immune compromised patients. The increase in prevalence and emergence of multidrug resistance among bacteria including methicillin-resistant *Staphylococcus aureus* (MRSA) has endangered the efficacy of antibiotics in the advent of modern medicine.[1] Antimicrobial resistant bacteria result in increased mortality rate and increased healthcare cost. According to a study by World Health Organization (WHO), microbial infection can become one of the most serious causes for human death in near future.[2] Considering these facts, there is an urgent need to develop new effective antibacterial agents that circumvent the emergence of resistance and thus, there have been tremendous efforts by researchers to find new antibiotics to combat microbial resistance.[3]

Nitrogen-containing heterocyclic compounds are the most abundant and integral scaffolds because of their distinct biological and industrial activities.[4] In the past, a number of indole and quinazoline-based compounds have been shown to be promising antimicrobial agents (Figure 1).[5] Hoemann et al. found that 2-(1*H*-indol-3-yl)quinolines (**I**) are effective against methicillin-resistant *S. aureus* with minimum inhibitory concentration (MIC) values <1.0 μg/mL.[6] Yu and group synthesized a series of 2-(indole-3-yl)-thiochroman-4-ones (**II**) and found that these indole derivatives show good in vitro antifungal activity with MIC in the range of 4−8 μg/mL.[7] The bis(indole)alkaloid, topsentin (**III**) has received growing attention for their interesting antibacterial properties.[8] Kung et al. found that quinazoline-derived compounds (**IV**) have exhibited good antibacterial activity against *Escherichia coli*, *S. aureus*, and *K. pneumonia* with MIC values ranging from 0.2−12 μM.[9] A few quinazoline-fused molecules such as indolo-, imidazo-, and benzimidazo-quinazolines have also been found to exhibit potential antifungal and antibacterial activities (Figure 1).[10] For example, indolo[1,2-*c*]quinazoline (**V**) has been found to possess good antimicrobial activity with MIC values ranging from 2.5−20 μg/mL.[10a] On the basis of the high degree of bioactivity shown by molecules based on indole, quinazoline, and imidazole moieties and also in continuation of our ongoing research interest for the synthesis of novel-fused heterocyclic molecules under mild reaction conditions,[11] we became interested toward designing a novel imidazo/benzimidazo[1,2-*c*]quinazoline structural framework (**8**) that incorporates all these three moieties into a single molecular framework and evaluate their potential additive effects on the antimicrobial activities.

Received: July 10, 2018
Accepted: October 19, 2018
Published: November 30, 2018

DOI: 10.1021/acsomega.8b01592
ACS Omega 2018, 3, 16338−16346

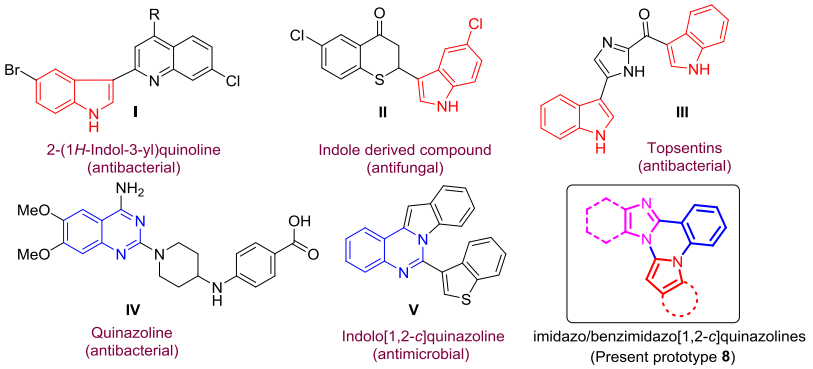

Figure 1. Antimicrobial agents with indole and quinazoline motifs and designed imidazo/benzimidazo[1,2-*c*]quinazolines.

2. RESULTS AND DISCUSSION

2.1. Chemistry. Initially, benzil and related dicarbonyl compounds (**1a**−**f**), 2-bromoaryl aldehyde (**2**), and ammonium acetate (**3**) were reacted in the presence of L-proline/MeOH to provide a series of 2-(2-bromoaryl)-1*H*-imidazole (**5a**−**f**) via a multicomponent strategy.[12] Similarly, the reaction of 2-bromoaryl aldehyde (**2**) with 1,2-diaminobenzene (**4**) in the presence of H_2O_2/CAN gave 2-(2-bromophenyl)-1*H*-benzo[*d*]imidazole (**5g**) (Scheme 1).[13]

Scheme 1. Synthesis of 2-(2-Bromoaryl)-1*H*-imidazole and 2-(2-Bromophenyl)-1*H*-benzo[*d*]imidazole

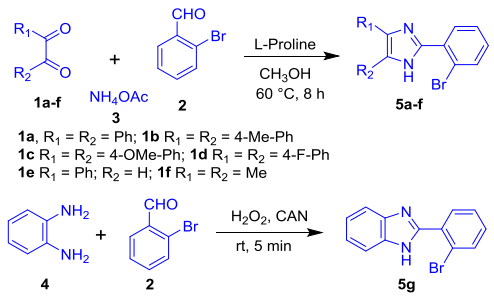

The designed prototype that is fused imidazo/benzimidazo quinazolines (**8**) were synthesized by using our previous approach with a slight modification in the reaction conditions.[13] Interestingly, in the present approach, we have successfully established copper-catalyzed cross-dehydrogenative coupling (CDC) instead of a palladium-catalyzed CDC strategy reported earlier. Copper-catalyzed Ullmann type C−N coupling between 2-(2-bromophenyl)-1*H*-imidazole/benzimidazole (**5**) with azoles (**6**) in the presence of CuI (20 mol %), K_2CO_3 in dimethylformamide (DMF) at 150 °C, followed by CDC in the presence of $Cu(OAc)_2{\cdot}H_2O$ resulted in the desired fused imidazo/benzimidazo quinazolines (**8**). As shown in Table 1, aryl substitution at C4 and C5- position on 2-(2-bromophenyl)-1*H*-imidazole was treated with different azoles such as 1,2,4-triazole, imidazole and indoles to afford corresponding imidazo[1,2-*c*]quinazolines (**8aa**−**ae**) in 40−65% yields. The 2-(2-bromophenyl)-1*H*-imidazole having different substituents such as -Me, -OMe and -F at the *p*-position of aryl ring at C4 and C5- position of imidazole smoothly reacted with imidazoles and pyrazole to give respective imidazo[1,2-*c*]quinazolines (**8bf**−**df**) in 45−60% yields. Similarly, the reaction of C4-arylated 2-(2-bromophenyl)-1*H*-imidazole with imidazole and benzimidazole produced corresponding imidazo[1,2-*c*]quinazolines (**8ef**−**eg**) in 62−70% yields. Furthemore, methyl substituted imidazole at C4 and C5- position well tolerated under standard reaction conditions and afforded the target product **8fb** in 45% yield. Similarly, 2-(2-bromophenyl)benzimidazole (**5g**) also reacted with different azoles (**6**) to afforded corresponding benzimidazo[1,2-*c*]quinazolines (**8gf**, **8ga**, **8gh**, **8gc**, **8gi**, and **8gd**) in 35−70% yields. The molecular structure of the synthesized imidazo/benzimidazo[1,2-*c*]quinazoline derivatives (**8**) was confirmed by ^{1}H and ^{13}C NMR and ESI-HRMS analysis.

2.2. Biology. *2.2.1. Antimicrobial Activity.* Antibacterial evaluation of imidazo/benzimidazo[1,2-*c*]quinazoline derivatives (**8**) was carried out against a panel of three Gram negative strains, viz., *E. coli*, *Pseudomonas putida* (*P. putida*), and *Salmonella typhi* (*S. typhi*) and two Gram positive strains, viz., *Bacillus subtilis* (*B. subtilis*) and *S. aureus* using ciprofloxacin as a standard drug. Antifungal efficacy was evaluated against pathogenic strains, viz., *Candida albicans* (*C. albicans*) and *Aspergillus niger* (*A. niger*) using amphotericin B as a positive control. The results of antimicrobial activity are presented in Table 2. Initially, to understand the antibacterial effect of the synthesized compounds, zone of inhibition (ZOI) was measured through the disc diffusion method. Presence of these compounds in the culture medium increased the ZOI diameter by 1 to 7 mm. Compounds **8ga**, **8gc**, and **8gd**, with an increase of 6−7 mm in the inhibition zone diameter were found to be the most promising candidate for antibacterial activity. Next, for quantitative measurement of the antibacterial activity of **8aa**−**gd**, MIC was evaluated. It was found that the compounds (**8aa**−**gd**) effectively inhibited the growth of pathogenic strains with MIC in the range of 4−64 μg/mL. Among all tested compounds, **8ga**, **8gc**, and **8gd** were found to be most effective compounds with MIC in the range of 4−8 μg/mL.

With respect to antifungal activity, compounds **8bf**, **8ef**, **8gf**, **8ga**, **8gh**, **8gc**, **8gi**, and **8gd** exhibited good to excellent activity against *A. niger* and *C. albicans*. Compounds **8bf**, **8ef**, and **8gh** were found equally potent (MIC in the range of 32 μg/mL) in comparison to the reference drug amphotericin B, whereas compounds **8gf**, **8ga**, **8gc**, **8gi**, and **8gd** even showed better activity than the positive control with MIC in the range of 8−16 μg/mL.

It was observed that benzimidazole derivatives substituted with indoles (**14gc**−**gd**) and azoles [1,2,4-triazole (**8ga**), imidazole (**8gf**), and pyrazole (**8gh**)] exhibited better antibacterial activity in comparison to the imidazole substrate containing similar motifs (**8aa**−**fb**). More specifically, benzimidazole fused with indole-bearing electron-withdrawing

DOI: 10.1021/acsomega.8b01592
ACS Omega 2018, 3, 16338−16346

Table 1. Synthesis of Fused Imidazo/Benzimidazo[1,2-*c*]quinazolines (8)[a,b]

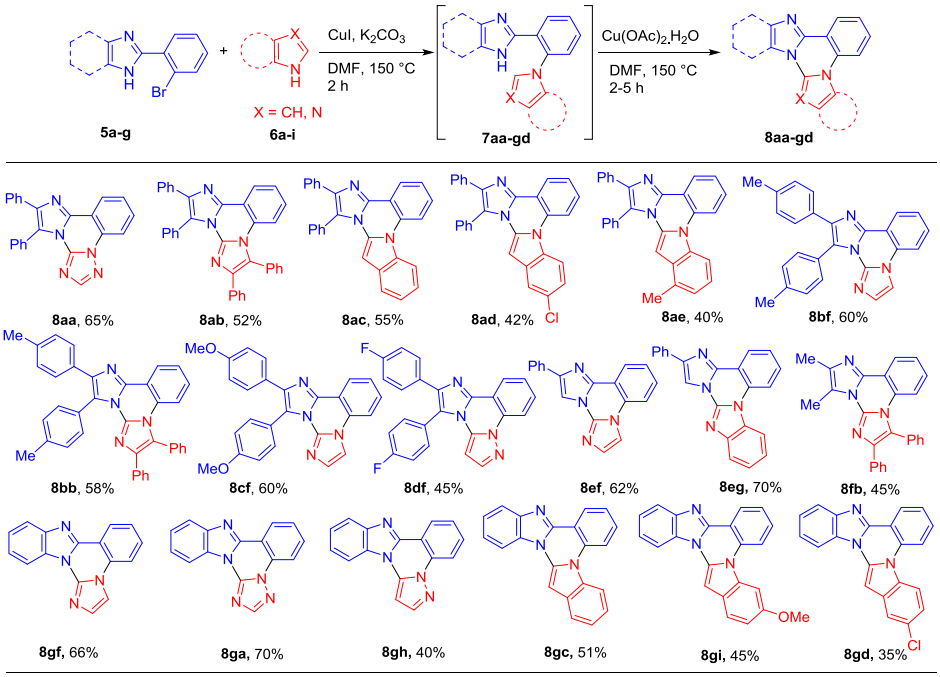

[a]Reaction conditions: **5** (1.0 mmol), **6** (1.2 mmol), CuI (20 mol %), K_2CO_3 (2.0 mmol), and DMF (2.0 mL) under air at 150 °C for 2 h followed by the addition of $Cu(OAc)_2{\cdot}H_2O$ (0.5 mmol), 150 °C, 2−5 h. [b]Isolated yield.

Table 2. Antimicrobial Activity of Fused Imidazo/Benzimidazo[1,2-*c*]quinazolines (8)[a]

	MIC (μg/mL)						
	Bacteria					fungi	
	Gram negative			Gram positive			
compounds	*E. coli*	*P. putida*	*S. typhi*	*B. subtilis*	*S. aureus*	*C. albicans*	*A. niger*
8aa	>32	>32	32	64	64	>32	>32
8ab	64	>32	64	32	32	[b]	[b]
8ac	64	>64	64	>64	64	128	>64
8ad	32	32	>32	32	32	[b]	[b]
8ae	>64	64	64	>32	>32	64	64
8bf	>32	32	>32	32	32	32	32
8bb	>16	32	32	>16	>16	>32	>32
8cf	32	>32	32	32	>32	>128	>128
8df	>16	16	16	>16	>16	64	>64
8ef	32	>32	>32	>32	>32	32	32
8eg	32	32	32	32	>32	64	64
8fb	64	64	>64	>32	>32	128	128
8gf	>8	**8**	>8	**8**	>8	**16**	**16**
8ga	**4**	**4**	**>4**	8	8	**8**	**>8**
8gh	16	16	16	16	16	32	32
8gc	**4**	**4**	8	**4**	**>4**	**8**	**8**
8gi	16	>16	>16	16	>16	>16	>16
8gd	**4**	**>4**	**4**	**>4**	**>4**	**16**	**16**
ciprofloxacin	6.25	6.25	6.25	6.25	6.25		
amphotericin B						30	30

[a]MIC: minimum inhibitory concentration in μg/mL. [b]No activity.

group (−Cl) exhibited comparatively better activity than the electron neutral or electron-donating (−OMe) group. Similarly, the benzimidazole substrate fused with indole and azoles (1,2,4-triazole, imidazole, and pyrazole) exhibited better antifungal activity in comparison to the imidazole substrate containing a similar scaffold.

2.2.2. Bactericidal Assay by Propidium Iodide. The propidium iodide (PI) dye penetrates only the damaged or compromised membrane and hence can be used to detect dead cells.[14] The dye PI intercalates with double-stranded DNA, and subsequent fluorescence detection allows assessment of the number of nonviable/dead cells.[15] The most potent com-

DOI: 10.1021/acsomega.8b01592
ACS Omega 2018, 3, 16338−16346

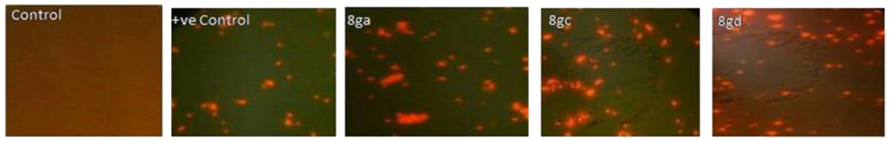

Figure 2. Bactericidal assay against *P. putida* for compounds **8ga**, **8gc**, and **8gd**.

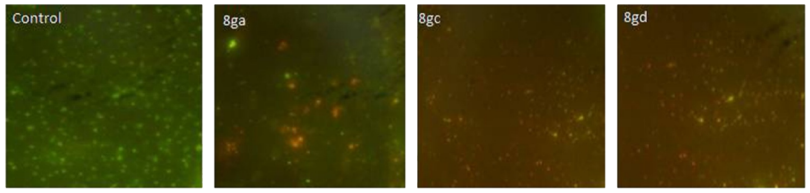

Figure 3. Live–dead bacterial cell screening by compounds **8ga**, **8gc**, and **8gd** using AO/Et·Br dual staining.

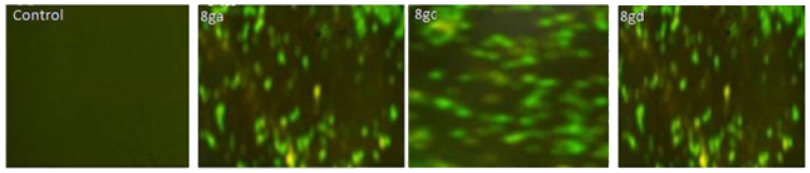

Figure 4. Evaluation of ROS production against *P. putida* using the fluorescent dye DCFH-DA as a probe.

pounds **8ga**, **8gc**, and **8gd** were further tested for their effect against the total cell population of *P. putida* using the PI dye. The microscopic images of the bacterial culture treated with the compounds showed significant cell death at 2× MIC, which is similar to the number of cells for the positive control treated with the *tert*-butyl hydroperoxide (TBHP) bacterial culture (Figure 2). The result revealed that the compounds **8ga**, **8gc**, and **8gd** have potent bactericidal activity.

2.2.3. Live–Dead Bacteria Cell Screening. Acridine orange (AO) is a vital dye and will stain both live and dead cells, whereas ethidium bromide (Et·Br) will stain only cells that have lost membrane integrity.[16] The cell death assay caused by most efficient compounds **8ga**, **8gc**, and **8gd** was evaluated by the AO/Et·Br dual staining assay (Figure 3). In this assay, *P. putida* cells were stained with a mixture of AO and Et·Br. The dye AO can enter inside living cells and binds with DNA of living cells to emit green fluorescence, whereas Et·Br enters only through the modified cell membrane of dead cells and emits red fluorescence. The untreated bacterial cells displayed green fluorescence, whereas the cells treated with compounds **8ga**, **8gc**, and **8gd** exhibited red fluorescence along with minor green fluorescence (Figure 3). This bacterial cell viability assay demonstrated that compounds **8ga**, **8gc**, and **8gd** cause cell damage by making loss of cell membrane integrity and thus illustrates the bactericidal potential of these compounds.

2.2.4. Evaluation of Reactive Oxygen Species Production. A moderate reactive oxygen species (ROS) generation plays a crucial role in cell proliferation and differentiation, whereas the excess production of ROS induces oxidative damage to cellular lipids, proteins, and DNA in bacteria which leads to cell death. Therefore, the effect of compounds **8ga**, **8gc**, and **8gd** on cellular ROS level of *P. putida* bacterial cells was measured using the 2′,7′-dichlorofluorescein diacetate dye (DCFH-DA). A significant increase in the ROS level was observed by the chemically synthesized compounds **8ga**, **8gc**, and **8gd** against *P. putida* cells (Figure 4). Compared to the untreated control cells, the compound-treated bacterial cell showed enhanced generation of intracellular ROS. This intracellular-accumulated ROS may also be responsible for bactericidal activity.

2.2.5. Hemolytic Activity. To ascertain the toxicity profile of synthesized compounds, hemolytic activity was evaluated. The hemolytic activity can occur by several mechanisms, from increased permeability of cell membranes to complete cell lysis. The evaluation of hemolytic activity is to check the damage caused by synthesized compounds to the membranes of RBCs (erythrocytes), which leads to release of hemoglobin. It is an additional tool to verify the importance of synthesized compounds against red blood cells (RBCs) and may also give an idea to promote such compounds as a drug level (Figure 5). The toxicity profile of chemically synthesized

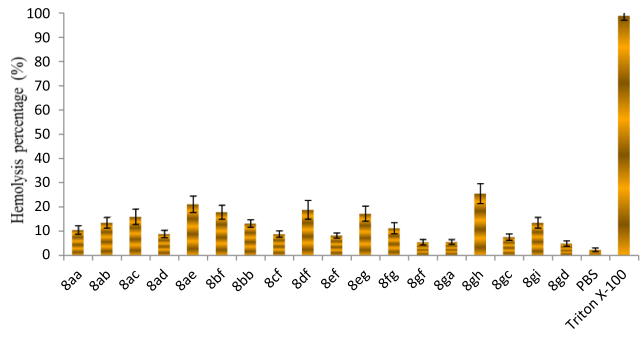

Figure 5. Hemolytic activity on human RBCs using **8aa**–**8gd** at 100 μM. Data were analyzed by mean ± SD (standard deviation) of triplicate (n = 3) samples.

compounds on human RBCs was determined at a fixed concentration of 100 μM. The observed results showed that most compounds caused 3–28% hemolysis. Interestingly, the efficient antibacterial compounds **8ga**, **8gc**, and **8gd** showed less than 10% hemolysis at a high concentration of 100 μM, suggesting that these compounds are negligibly toxic to human blood cells (Figure 5). The results of hemolytic activity further support the significance of the present study.

DOI: 10.1021/acsomega.8b01592
ACS Omega 2018, 3, 16338–16346

After the preliminary hemolytic activity of tested compounds at 100 μM concentration, the concentration-dependent activity of one of the most potent compounds **8ga** was performed at different concentrations (20−100 μM). It was found that the hemolysis activity of **8ga** increased with increasing concentration and was less than 10% hemolysis for the concentration range of 20−100 μM. The observed results of compound **8ga** at different concentrations showed its negligible toxicity to human blood cells (Figure 6).

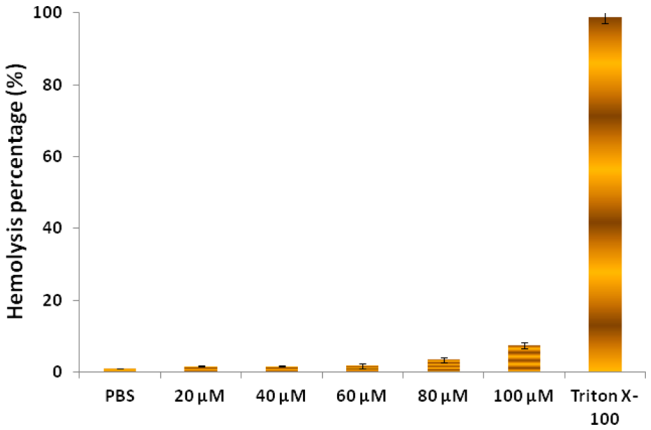

Figure 6. Hemolytic activity of compound **8ga** on human RBCs at different concentrations 20−100 μM. Data were analyzed by mean ± SD (standard deviation) of triplicate (n = 3) samples.

2.2.6. Biofilm Inhibition. Bacterial biofilm is an extracellular polymeric substance and composed of extracellular polysaccharides and proteins, causing chronic infections in humans via hospital and community environments. Biofilm formation provides resistance to microbes against phagocytosis and other components of the body's defense system. Thus, compounds having antibiofilm activity could prevent the contamination of biomedical implants. In our study, we observed that most of the compounds showed antibiofilm activity in the range of 20−70%, as compared to positive control ciprofloxacin (Figure 7).

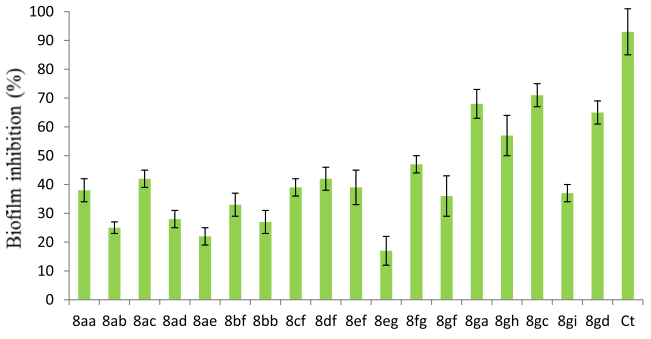

Figure 7. Biofilm inhibition assay against strain *S. aureus* by **8aa−8gd** at 50 μg/mL. All experiments were carried out in triplicates, and the values are indicated as mean ± SD.

The highest inhibitory activity was shown by compounds **8gc** (70%), followed by **8ga** (67%) and **8gd** (63%) (Figure 7). Compounds can modulate the biofilm formation through the nonmicrobicidal or biocidal mechanism. Moreover, these molecules weaken the biofilm either by degradation of the extracellular matrix or targeting of extracellular and intracellular signaling molecules.

The analysis of antibacterial activity confirmed their efficacy against tested bacteria because of damage on the bacterial membranes and the effects of oxidative stress as evident by the live−dead bacterial assay and ROS production, respectively. Generation of ROS leads to a lethal effect on bacterial cells and can increase the bactericidal process. The acute change in response to compound treatment may cause the release and degradation of membrane proteins; this leads to the loss of membrane integrity and bacterial cell morphology, formation of fissures, and perforations in the cell membrane. The formation of fissures and perforation leads to the leakage of cytoplasmic contents from the cell; this increases the death consequences.

The overall study concludes that benzimidazole derivatives bearing the indole, 1,2,4-triazole, imidazole, and pyrazole group induced greater oxidative stress and morphological changes like membrane damage. Moreover, pathological outcomes such as DNA damage, alterations to specific proteins, and enzymes responsible for different physiological processes at the molecular level need further investigation.

3. CONCLUSIONS

A new series of imidazo/benzimidazo[1,2-*c*]quinazolines has been synthesized via copper-catalyzed Ullmann type C−N coupling followed by the intramolecular CDC reaction. All of the synthesized compounds were evaluated for their antimicrobial activity. Among all, compounds **8gf**, **8ga**, **8gc**, and **8gd** exhibited most promising antibacterial (MIC 4−8 μg/mL) and antifungal (MIC 4−16 μg/mL) activities. The structure activity relationship of synthesized compounds revealed that benzimidazo[1,2-*c*]quinazolines showed better antimicrobial activity than imidazo[1,2-*c*]quinazoline derivatives. Among benzimidazo[1,2-*c*]quinazolines, 1,2,4-triazole (**8ga**) and indole (**8gc** and **8gd**)-fused benzimidazo[1,2-*c*]quinazolines exhibited better antimicrobial activity as compared to other azoles. The live−dead bacteria cell screening and increased ROS production upon treatment with most active compounds **8ga**, **8gc**, and **8gd**, illustrates their efficient membrane penetration ability which might be the main cause of bacterial cell death. Furthermore, synthesized compounds were also evaluated for hemolytic activity which showed a negligible toxicity profile toward human blood cells. The overall study concludes that compounds **8ga**, **8gc**, and **8gd** may serve as potential antimicrobial candidates for lead optimization.

4. EXPERIMENTAL SECTION

All reagents and solvents were obtained from commercial suppliers and used without further purification unless otherwise mentioned. Progress of the reactions was monitored by using thin layer chromatography (TLC) on 0.2 mm silica gel F_{254} plates. The chemical structures of the final products were determined by the NMR (^{1}H and ^{13}C) and HRMS analysis. ^{1}H NMR and ^{13}C NMR spectra were recorded on a 400 and 100 MHz spectrometer. Chemical shifts are reported in parts per million (ppm) using tetramethylsilane as an internal standard or the deuterated solvent peak ($CDCl_3$ and DMSO-d_6). HRMS data were recorded on a mass spectrometer with an electrospray ionization and TOF mass analyzer. Melting points were determined in open capillary tubes on an automated melting point apparatus and are uncorrected. All tested compounds were ≥95% pure by high-

DOI: 10.1021/acsomega.8b01592
ACS Omega 2018, 3, 16338−16346

performance liquid chromatography (HPLC) with detection at 270 nm. Starting substrates 2-(2-bromophenyl)-4,5-diaryl-1*H*-imidazole and 2-(2-bromophenyl)-1*H*-benzo[*d*]imidazole were prepared by the following reported procedure.[12,13]

4.1. General Procedure for the Synthesis of Imidazo/Benzimidazo[1,2-*c*]quinazolines. A clean oven-dried 10 mL round-bottom flask was charged with **5** (1.0 mmol), **6** (1.2 mmol), K_2CO_3 (2.0 mmol), CuI (0.20 mmol), and DMF (2 mL). The resulting solution was stirred at 150 °C for 2 h. On completion of the first step monitored by TLC, $Cu(OAc)_2 \cdot H_2O$ (0.5 mmol) was added in the same flask without isolating the intermediate, and the reaction mass was further stirred at 150 °C for 2−5 h. The reaction progress was monitored by TLC. After completion, the reaction mass was allowed to cool at ambient temperature, diluted with water (10 mL), and extracted with EtOAc (2 × 10 mL). The combined organic layer was dried over anhydrous Na_2SO_4 and concentrated under reduced pressure. The crude material was purified by column chromatography on silica gel (100−200 mesh) using ethyl acetate/hexane (15%, v/v) as an eluant.

*4.1.1. 5,6-Diphenylimidazo[1,2-c][1,2,4]triazolo[1,5-a]quinazoline (**8aa**).* Off-white solid; yield 65%; mp 260−261 °C (lit. = 260−261 °C);[13] ^{1}H NMR (400 MHz, $CDCl_3$): δ 8.75 (d, J = 8.0 Hz, 1H), 8.31 (d, J = 8.3 Hz, 1H), 8.05 (s, 1H), 7.78 (t, J = 7.6 Hz, 1H), 7.69−7.56 (m, 8H), 7.33−7.29 (m, 3H); ^{13}C NMR (100 MHz, $CDCl_3$): δ 151.2, 143.8, 142.0, 140.4, 133.2, 131.8, 130.8, 130.7, 129.5, 129.0, 128.5, 128.3, 127.9, 127.7, 127.0, 124.7, 115.5, 114.6; HRMS (ESI): calcd for $C_{23}H_{16}N_5$, 362.1400; found, 362.1400 $[M + H]^+$.

*4.1.2. 2,3,6,7-Tetraphenyldiimidazo[1,2-a:1′,2′-c]quinazoline (**8ab**).* Off-white solid; yield 52%; mp 255−257 °C; ^{1}H NMR (400 MHz, $CDCl_3$): δ 8.73 (d, J = 7.9 Hz, 1H), 7.77−7.71 (m, 4H), 7.65−7.57 (m, 8H), 7.43 (t, J = 7.6 Hz, 1H), 7.35−7.28 (m, 3H), 7.23−7.12 (m, 6H), 6.93 (d, J = 8.6 Hz, 1H); ^{13}C NMR (100 MHz, $CDCl_3$): δ 141.2, 139.8, 136.7, 136.7, 133.8, 133.6, 132.2, 132.1, 132.0, 131.8, 130.5, 130.0, 129.3, 128.8, 128.3, 128.0, 128.0, 127.8, 127.3, 126.9, 126.6, 125.4, 125.2, 125.0, 122.6, 116.0, 115.9; HRMS (ESI): calcd for $C_{36}H_{25}N_4$, 513.2074; found, 513.2073 $[M + H]^+$.

*4.1.3. 1,2-Diphenylimidazo[1,2-c]indolo[1,2-a]quinazoline (**8ac**).* Off-white solid; yield 55%; mp 240−243 °C; ^{1}H NMR (400 MHz, $CDCl_3$): δ 8.71 (dd, J = 7.9, 1.6 Hz, 1H), 8.47 (d, J = 8.5 Hz, 1H), 8.29 (d, J = 8.4 Hz, 1H), 7.70−7.66 (m, 4H), 7.63−7.61 (m, 4H), 7.51−7.45 (m, 2H), 7.39−7.34 (m, 1H), 7.32−7.30 (m, 2H), 7.26−7.23 (m, 2H), 5.48 (s, 1H); ^{13}C NMR (100 MHz, $CDCl_3$): δ 140.9, 139.1, 134.2, 133.8, 131.9, 131.7, 130.9, 130.7, 130.1, 129.8, 129.1, 128.8, 128.3, 127.3, 127.2, 125.3, 125.0, 124.0, 122.4, 122.3, 121.0, 115.2, 113.4, 87.9; HRMS (ESI): calcd for $C_{29}H_{20}N_3$, 410.1652; found, 410.1672 $[M + H]^+$.

*4.1.4. 11-Chloro-1,2-diphenylimidazo[1,2-c]indolo[1,2-a]quinazoline (**8ad**).* Brown solid; yield 42%; mp 259−261 °C; ^{1}H NMR (400 MHz, $CDCl_3$): δ 8.73 (d, J = 7.8 Hz, 1H), 8.37 (d, J = 8.5 Hz, 1H), 8.18 (d, J = 9.0 Hz, 1H), 7.70−7.60 (m, 8H), 7.51−7.47 (m, 2H), 7.32−7.28 (m, 4H), 5.41 (s, 1H); ^{13}C NMR (100 MHz, $CDCl_3$): δ 141.0, 139.0, 133.8, 133.6, 132.7, 131.8, 130.5, 130.2, 130.1, 129.9, 129.2, 128.3, 128.0, 127.3, 125.4, 125.0, 124.4, 122.3, 120.3, 115.3, 115.0, 114.3, 87.3; HRMS (ESI): calcd for $C_{29}H_{19}ClN_3$, 444.1262; found, 444.1237 $[M + H]^+$.

*4.1.5. 12-Methyl-1,2-diphenylimidazo[1,2-c]indolo[1,2-a]quinazoline (**8ae**).* White solid; yield 40%; mp 272−274 °C; ^{1}H NMR (400 MHz, $CDCl_3$): δ 8.57 (d, J = 7.8 Hz, 1H), 8.35 (d, J = 8.5 Hz, 1H), 8.24 (d, J = 8.4 Hz, 1H), 7.54−7.30 (m, 15H), 1.47 (s, 3H); ^{13}C NMR (100 MHz, $CDCl_3$): δ 134.3, 132.4, 131.0, 130.9, 130.7, 130.2, 128.9, 128.4, 128.2, 127.2, 126.3, 125.2, 123.6, 123.0, 122.2, 119.0, 115.3, 114.6, 113.8, 99.9, 9.3; HRMS (ESI): calcd for $C_{30}H_{22}N_3$, 424.1808; found, 424.1808 $[M + H]^+$.

*4.1.6. 2,3-Di-p-tolyldiimidazo[1,2-a:1′,2′-c]quinazoline (**8bf**).* Brown solid; yield 60%; mp 224−226 °C (lit. = 224 °C);[13] ^{1}H NMR (300 MHz, $CDCl_3$): δ 8.70 (d, J = 7.8 Hz, 1H), 7.70−7.60 (m, 3H), 7.55−7.47 (m, 5H), 7.3 (d, J = 7.8 Hz, 2H), 7.18 (s, 1H), 7.10 (d, J = 7.9 Hz, 2H), 2.49 (s, 3H), 2.35 (s, 3H); ^{13}C NMR (75 MHz, $CDCl_3$): δ 141.4, 139.5, 138.7, 137.3, 137.0, 131.6, 130.9, 130.3, 129.9, 129.1, 129.0, 128.9, 127.7, 127.0, 126.0, 125.2, 124.6, 115.2, 114.6, 109.9, 21.7, 21.3; HRMS (ESI): calcd for $C_{26}H_{21}N_4$, 389.1761; found, 389.1771 $[M + H]^+$.

*4.1.7. 6,7-Diphenyl-2,3-di-p-tolyldiimidazo[1,2-a:1′,2′-c]quinazolines (**8bb**).* White solid; yield 58%; mp 251−253 °C; ^{1}H NMR (400 MHz, $CDCl_3$): δ 8.73 (d, J = 7.9 Hz, 1H), 7.70−7.57 (m, 9H), 7.42−7.37 (m, 4H), 7.25−7.15 (m, 7H), 6.94 (d, J = 8.7 Hz, 1H), 2.57 (s, 3H), 2.38 (s, 3H); ^{13}C NMR (100 MHz, $CDCl_3$): δ 141.1, 139.6, 138.5, 137.0, 136.7, 136.7, 133.7, 132.2, 132.1, 131.9, 131.8, 131.1, 129.9, 129.9, 129.1, 129.0, 128.7, 128.0, 127.7, 126.8, 126.7, 125.4, 125.2, 124.8, 122.52, 116.0, 115.9, 21.6, 21.3; HRMS (ESI): calcd for $C_{38}H_{29}N_4$, 541.2387; found, 541.2382 $[M + H]^+$.

*4.1.8. 2,3-Bis(4-methoxyphenyl)diimidazo[1,2-a:1′,2′-c]quinazoline (**8cf**).* Brown solid; yield 60%; mp 223 °C (lit. = 223 °C);[13] ^{1}H NMR (300 MHz, $CDCl_3$): δ 8.69 (d, J = 7.8 Hz, 1H), 7.70−7.49 (m, 8H), 7.18−7.16 (m, 1H), 7.03 (d, J = 7.8 Hz, 2H), 6.84 (d, J = 8.0 Hz, 2H), 3.91 (s, 3H), 3.81 (s, 3H); ^{13}C NMR (75 MHz, $CDCl_3$): δ 159.9, 158.9, 141.0, 139.3, 137.2, 133.1, 130.3, 129.9, 129.0, 128.8, 126.3, 126.0, 125.2, 123.8, 122.0, 115.0, 114.6, 113.8, 113.7, 109.9, 55.2, 55.2; HRMS (ESI): calcd for $C_{26}H_{21}N_4O_2$, 421.1659; found, 421.1676 $[M + H]^+$.

*4.1.9. 2,3-Bis(4-fluorophenyl)imidazo[1,2-c]pyrazolo[1,5-a]quinazoline (**8df**).* Off-white solid; yield 45%; mp 257−260 °C; ^{1}H NMR (400 MHz, $CDCl_3$ + formic acid): δ 8.60 (d, J = 8.0 Hz, 1H), 8.36 (d, J = 8.3 Hz, 1H), 7.78−7.74 (m, 2H), 7.62−7.51 (m, 5H), 7.30 (t, J = 8.5 Hz, 2H), 7.03 (t, J = 8.6 Hz, 2H), 5.41 (d, J = 2.3 Hz, 1H); ^{13}C NMR (100 MHz, $CDCl_3$): δ 163.9 (d, J = 252.0 Hz), 162.8 (d, J = 249.0 Hz), 141.5, 139.2, 138.7, 133.7 (d, J = 8.4 Hz), 133.4, 132.6, 132.1, 130.0 (d, J = 8.3 Hz), 127.0, 126.9, 124.7, 123.9 (d, J = 3.6 Hz), 123.4, 116.8 (d, J = 21.8 Hz), 115.7 (d, J = 21.7 Hz), 115.6, 112.3, 92.5; HRMS (ESI): calcd for $C_{24}H_{15}F_2N_4$, 397.1259; found, 397.1262 $[M + H]^+$.

*4.1.10. 2-Phenyldiimidazo[1,2-a:1′,2′-c]quinazoline (**8ef**).* Off-white solid; yield 62%; mp 190 °C (lit. = 188−190 °C);[13] ^{1}H NMR (400 MHz, $CDCl_3$): δ 8.55 (d, J = 7.6 Hz, 1H), 8.24 (s, 1H), 7.99 (d, J = 7.3 Hz, 2H), 7.66 (d, J = 1.32 Hz, 1H), 7.63−7.53 (m, 2H), 7.50−7.45 (m, 3H), 7.36 (t, J = 7.3 Hz, 1H), 7.31 (d, J = 1.6 Hz, 1H); ^{13}C NMR (100 MHz, $CDCl_3$): δ 144.6, 140.2, 136.6, 133.1, 130.3, 130.0, 128.8, 128.7, 127.9, 126.0, 125.8, 125.1, 114.8, 114.7, 110.7, 108.0; HRMS (ESI): calcd for $C_{18}H_{13}N_4$, 285.1135; found, 285.1112 $[M + H]^+$.

*4.1.11. 2-Phenylbenzo[4,5]imidazo[1,2-a]imidazo[1,2-c]quinazoline (**8eg**).* Brown solid; yield 70%; mp 208−210 °C; ^{1}H NMR (400 MHz, $CDCl_3$): δ 8.70 (dd, J = 7.9, 1.6 Hz, 1H), 8.40 (s, 1H), 8.37 (d, J = 8.4 Hz, 1H), 8.19 (dd, J = 7.6, 1.7 Hz, 1H), 8.04 (dd, J = 8.4, 1.5 Hz, 2H), 7.92−7.90 (m, 1H), 7.77−7.73 (m, 1H), 7.59−7.55 (m, 1H), 7.52−7.47 (m,

DOI: 10.1021/acsomega.8b01592
ACS Omega 2018, 3, 16338−16346

4H), 7.41−7.37 (m, 1H); ^{13}C NMR (100 MHz, $CDCl_3$): δ 145.4, 142.0, 141.2, 140.8, 132.8, 132.7, 130.9, 130.6, 128.9, 128.2, 125.9, 125.5, 125.4, 124.6, 123.3, 120.0, 115.0, 114.9, 113.1, 108.8; HRMS (ESI): calcd for $C_{22}H_{15}N_4$, 335.1291; found, 335.1287 $[M + H]^+$.

*4.1.12. 2,3-Dimethyl-6,7-diphenyldiimidazo[1,2-a:1′,2′-c]-quinazoline (**8fb**).* White solid; yield 45%; mp 271−273 °C; ^{1}H NMR (400 MHz, $CDCl_3$):δ 8.49 (dd, *J* = 8.0, 1.6 Hz, 1H), 7.65−7.56 (m, 7H), 7.35 (t, *J* = 7.5 Hz, 1H), 7.26−7.22 (m, 3H), 7.15−7.10 (m, 1H), 6.93 (d, *J* = 8.6 Hz, 1H), 3.00 (s, 3H), 2.46 (s, 3H); ^{13}C NMR (100 MHz, $CDCl_3$):δ 138.3, 137.8, 137.5, 137.2, 133.8, 132.0, 131.8, 131.6, 129.8, 128.4, 128.2, 127.1, 127.0, 125.4, 124.3, 122.5, 121.4, 116.0, 116.0, 12.9, 11.2; HRMS (ESI): calcd for $C_{26}H_{21}N_4$, 389.1761; found, 389.1777 $[M + H]^+$.

*4.1.13. Benzo[4,5]imidazo[1,2-c]imidazo[1,2-a]-quinazoline (**8gf**).* Brown solid; yield 66%; mp 192−195 °C (lit. = 192−195 °C);[13] ^{1}H NMR (400 MHz, $CDCl_3$): δ 8.72−8.69 (m, 1H), 8.64−8.61 (m, 1H), 8.00−7.98 (m, 1H), 7.72−7.71 (m, 3H), 7.58−7.52 (m, 3H), 7.42 (d, *J* = 1.7 Hz, 1H); ^{13}C NMR (100 MHz, $CDCl_3$) δ 143.9, 143.4, 137.7, 132.0, 131.8, 129.8, 129.0, 126.5, 126.2, 125.0, 124.2, 119.6, 114.9, 114.6, 114.3, 110.1; HRMS (ESI): calcd for $C_{16}H_{11}N_4$, 259.0978; found, 259.0972 $[M + H]^+$.

*4.1.14. Benzo[4,5]imidazo[1,2-c][1,2,4]triazolo[1,5-a]-quinazoline (**8ga**).* Off-white solid; yield 70%; mp 170−172 °C (lit. = 170−172 °C);[13] ^{1}H NMR (300 MHz, $CDCl_3$): δ 8.60 (d, *J* = 7.9 Hz, 1H), 8.39−8.36 (m, 1H), 8.20−8.17 (m, 2H), 7.92−7.89 (m, 1H), 7.75 (t, *J* = 7.5 Hz, 1H), 7.57 (t, *J* = 7.7 Hz, 1H), 7.50−7.48 (m, 2H); ^{13}C NMR (75 MHz, $CDCl_3$): δ 151.5, 144.1, 143.9, 143.5, 132.3, 132.1, 129.2, 127.1, 125.8, 125.6, 124.6, 120.0, 115.6, 114.0, 113.6; HRMS (ESI): calcd for $C_{15}H_{10}N_5$, 260.0931; found, 260.0941 $[M + H]^+$.

*4.1.15. Benzo[4,5]imidazo[1,2-c]pyrazolo[1,5-a]-quinazoline (**8gh**).* Off-white solid; yield 40%; mp 146−148 °C; ^{1}H NMR (400 MHz, $CDCl_3$): δ 8.65 (dd, *J* = 7.8, 1.4 Hz, 1H), 8.38 (dd, *J* = 8.4, 1.1 Hz, 1H), 8.01−7.99 (m, 2H), 7.87−7.85 (m, 1H), 7.80−7.75 (m, 1H), 7.58−7.50 (m, 3H), 6.77 (d, *J* = 2.1 Hz, 1H); ^{13}C NMR (100 MHz, $CDCl_3$): δ 143.8, 143.8, 141.9, 134.4, 133.9, 132.3, 129.9, 126.2, 125.8, 124.8, 123.9, 120.3, 115.5, 113.6, 111.3, 90.4; HRMS (ESI): calcd for $C_{16}H_{11}N_4$, 259.0978; found, 259.1002 $[M + H]^+$.

*4.1.16. Benzo[4,5]imidazo[1,2-c]indolo[1,2-a]-quinazolines (**8gc**).* Off-white solid; yield 51%; mp 178−180 °C; ^{1}H NMR (400 MHz, $CDCl_3$): δ 8.65 (d, *J* = 7.8 Hz, 1H), 8.34 (d, *J* = 8.5 Hz, 1H), 8.15 (d, *J* = 7.7 Hz, 1H), 7.98−7.93 (m, 2H), 7.72−7.66 (m, 2H), 7.50−7.48 (m, 2H), 7.41 (t, *J* = 7.6 Hz, 1H), 7.34−7.31 (m, 2H), 6.86 (s, 1H); ^{13}C NMR (100 MHz, $CDCl_3$): δ 144.2, 144.0, 135.6, 131.9, 131.8, 130.9, 130.7, 129.4, 126.6, 124.4, 124.0, 123.7, 122.6, 122.4, 120.8, 120.0, 115.3, 114.3, 113.3, 112.1, 86.4; HRMS (ESI): calcd for $C_{21}H_{14}N_3$, 308.1182; found, 308.1165 $[M + H]^+$.

*4.1.17. 3-Methoxybenzo[4,5]imidazo[1,2-c]indolo[1,2-a]-quinazoline (**8gi**).* White solid; yield 45%; mp 198−200 °C; ^{1}H NMR (400 MHz, $CDCl_3$): δ 8.72 (dd, *J* = 7.9, 1.6 Hz, 1H), 8.38 (d, *J* = 8.5 Hz, 1H), 8.14 (d, *J* = 9.1 Hz, 1H), 8.04−8.00 (m, 2H), 7.76−7.72 (m, 1H), 7.54−7.52 (m, 2H), 7.46 (t, *J* = 7.5 Hz, 1H), 7.24 (d, *J* = 2.6 Hz, 1H), 7.01 (dd, *J* = 9.1, 2.6 Hz, 1H), 6.92 (s, 1H), 3.95 (s, 3H); ^{13}C NMR (100 MHz, $CDCl_3$): δ 155.7, 144.2, 144.2, 135.5, 132.4, 132.0, 130.7, 130.6, 126.7, 125.9, 124.5, 123.9, 123.6, 120.0, 114.9, 114.2, 112.1, 111.3, 103.0, 86.4, 55.7; HRMS (ESI): calcd for $C_{22}H_{16}N_3O$, 338.1288; found, 338.1285 $[M + H]^+$.

*4.1.18. 2-Chlorobenzo[4,5]imidazo[1,2-c]indolo[1,2-a]-quinazoline (**8gd**).* Off-white solid; yield 35%; mp 245−247 °C; ^{1}H NMR (400 MHz, $CDCl_3$): δ 8.64 (d, *J* = 7.8 Hz, 1H), 8.23 (d, *J* = 8.5 Hz, 1H), 8.04 (d, *J* = 9.0 Hz, 1H), 7.96 (d, *J* = 7.2 Hz, 1H), 7.88 (d, *J* = 7.4s Hz, 1H), 7.68 (t, *J* = 7.2 Hz, 1H), 7.63 (d, *J* = 2.2 Hz, 1H), 7.53−7.47 (m, 2H), 7.43 (t, *J* = 7.6 Hz, 1H), 7.26−7.25 (m, 1H), 6.76 (s, 1H); ^{13}C NMR (100 MHz, $CDCl_3$): δ 144.1, 143.8, 135.0, 132.7, 132.0, 130.6, 130.6, 129.2, 128.2, 126.7, 124.6, 124.5, 123.9, 122.4, 120.1, 115.0, 114.3, 114.2, 112.04, 85.7; HRMS (ESI): calcd for $C_{21}H_{13}ClN_3$, 342.0793; found, 342.0799 $[M + H]^+$.

4.2. Antimicrobial Activity. *4.2.1. Antibacterial Activity.* The compounds **8** were tested for antibacterial activity against three Gram negative bacteria including *E. coli* (MTCC 1652), *P. putida* (MTCC 102), and *S. typhi* (98) and two Gram positive bacteria including *B. subtilis* (MTCC 121) and *S. aureus* (MTCC 96) as per the standard method.[17] The tested strains were collected from the Microbial Type Culture Collection and Gene Bank (MTCC, India). The autoclaved Luria−Bertani agar medium was poured into sterile glass Petri dishes (90 mm) under aseptic conditions. After solidification of the medium, 100 μL culture of each pathogenic culture (10^7 cfu/mL) was spread using a sterile glass spreader and left for 15 min for complete adsorption. After adsorption, a well size of 6 mm diameter was made by the sterile metallic borer, and the solution of the working compound of different concentrations was poured into the wells. After incubation at 37 °C for 24 h, the diameter of ZOI was measured in comparison with standard antibiotic "ciprofloxacin". The solvent, DMSO was used as the negative control, whereas antibiotic "ciprofloxacin" as the positive control. For the MIC assay, test compounds were prepared in concentrations of 2, 4, 8, 16, 32, 64, 128, and 256 μg/mL in DMSO and serial diluted test samples of each compound (200 μL) were added in 96-well microtrays. The test microorganism was added to microtrays well to obtain a final volume of 400 μL and incubated at 37 °C for 24 h. The MIC value is defined as the lowest concentration of the compound that inhibits the visible growth of bacteria (OD_{600} less than 0.06). Each assay was performed in duplicate sets.

4.2.2. Antifungal Activity. The compounds **8** were tested for antifungal activity by the agar well diffusion method against the fungal strains *C. albicans* (MTCC 3958) and *A. niger* (MTCC 9933). For the experimental work, a loopful of each strain was grown in the potato dextrose broth (PDB, HiMedia, India) medium at 28 °C for 4−5 days. Following optimal growth of each fungal strain, 100 μL of culture was uniformly spread on the potato dextrose agar medium plate. Following adsorption, wells of 6 mm were prepared by the sterile metallic borer and a solution of the working compound of different concentrations was poured into the wells. Plates were incubated at 28 °C for 4−5 days under dark conditions. The mean diameter of the inhibition zone was measured to determine antifungal activity. For the MIC assay, sterile test tubes containing 5 mL of sterilized Czapeks Dox broth medium was inoculated with 100 μL of freshly grown culture of each test strain and appropriate amount of the compound was added to achieve the desired concentrations. The tubes were incubated at 28 °C for five days under dark conditions and carefully observed for the presence of turbidity. Amphotericin B was used as the positive control. The experiment was performed in duplicate sets.

DOI: 10.1021/acsomega.8b01592
ACS Omega 2018, 3, 16338−16346

4.3. Bactericidal Assay by PI. The single colony of bacterium *P. putida* was inoculated into the sterile nutrient broth medium and kept in an incubator shaker (150 rpm) till the optical density (OD) of the culture reached up to 0.8. The culture was treated with selected compounds at 2× MIC for 4 h. After treatment, the culture was centrifuged at 5000*g* for 10 min, and the cell pellet was stained with 1.0 mg/mL of PI (Sigma-Aldrich, USA). The stained colony was streaked on the clean glass slide and covered with a glass slip. The population of PI-positive bacterial cells was compared with untreated cells by epifluorescence microscopy. During the experiment, the bacterial culture treated with TBHP was taken as the positive control.

4.4. Live−Dead Bacteria Screening through Fluorescence Microscopy. To discriminate live and dead bacterial cells, freshly grown culture of *P. putida* (10^7 cfu mL^{-1}) was treated with compounds **8ga**, **8gc**, and **8gd** for 4 h. Following treatment, 5 μL each of AO (15 μg mL^{-1}) and Et·Br (50 μg mL^{-1}) was added in a 500 μL of the *P. putida* culture. The working solution of acridine orange and ethidium bromide were prepared in the phosphate buffer saline (PBS) buffer. The suspension was centrifuged at 5000*g* for 10 min, and the supernatant was discarded. The cell pellet was washed with the 1× PBS buffer (pH 7.2) three times to remove any traces of unbound dyes. The washed cell pellet was streaked on the glass slide with a cover slip on top of it and viewed under an epifluorescence microscope (Olympus-CKX41, Olympus, Japan) at intensity between 450 and 490 nm using a 100× objective lens and 10× eyepiece lens.

4.5. Evaluation of ROS Production. To evaluate the intracellular reactive oxygen species formation after compound treatment, fluorescent dye DCFH-DA was used as probes. The DCFH is a nonfluorescent dye, but is oxidized to the highly fluorescent 2′,7′-dichlorofluorescein (DCF) by intracellular H_2O_2 or nitric oxide. At the mid log phase of bacterial growth, compounds were added to the bacterial suspension (*P. putida*) for 2 h and then treated with 2 μM of DCFH-DA at 37 °C for 30 min. The emitted fluorescence of DCF was measured at 530 nm after excitation at 485 nm by fluorescence microscopy and qualitatively screened for ROS production.

4.6. Hemolytic Activity. The compounds **8** were tested for hemolytic activity on human RBCs following the standard protocol with minor modifications.[18] The healthy human blood samples of males between 25 and 28 age groups were collected from the hospital of BITS Pilani campus following Institutional Ethics Committee guidelines and washed with the sterile PBS solution at least three times. After washing, blood was centrifuged at 2500 rpm for 6 min at room temperature and RBC pellet was suspended in the PBS buffer. The RBC suspension of 0.1 mL was mixed with 0.5 mL buffer solution containing 100 μg/mL of each compound in DMSO (1%, v/v) in the PBS buffer. DMSO (1%, v/v) in the PBS buffer and Triton X-100 (1%) were used as negative and positive controls, respectively. The samples were incubated at room temperature for 3 h. Following incubation, samples were centrifuged at 8000 rpm and absorbance of the supernatant was recorded at 540 nm. The percentage hemolysis was calculated by using the following equation:

[% Hemolysis = (A_{540} test sample − A_{540} negative control/ A_{540} positive control − absorbance 540 negative control) × 100]. Each sample was analyzed in triplicate sets.

4.7. Biofilm Inhibition Assay. The pathogenic bacterial strain *S. aureus* was cultured in the tryptic soy broth medium and OD of the bacterial suspension was adjusted to 1×10^6 cfu mL^{-1}. The synthesized compounds having concentrations of 50 μg/mL were mixed to the grown bacterial culture and properly mixed. The aliquots of 100 μL were distributed into the 96-well polystyrene microtiter plates (Tarson, India) and kept under static conditions at 37 °C for 24 h. The medium was discarded with micropipettes, and the plate was washed with PBS buffer (1×, pH 7.2) to wash away the nonadherent bacterial culture. The well of microtiter plates were stained with 100 μL of 0.1% crystal violet solution for 30 min at room temperature. After incubation, the staining solution was discarded, and wells were washed with autoclaved Milli-Q water and kept for air drying at room temperature. The stained biofilm were solubilized with 100 μL of 95% ethanol and absorbance was taken at 540 nm. Blank wells were taken as the background control. All experiments were carried out in triplicates, and the values are indicated as mean ± SD.

■ ASSOCIATED CONTENT

Supporting Information

The Supporting Information is available free of charge on the ACS Publications website at DOI: 10.1021/acsomega.8b01592.

Copies of ^{1}H and ^{13}C NMR, ESI-HRMS, and HPLC purity spectra of compounds **8aa**−**8gd** (PDF)

■ AUTHOR INFORMATION

Corresponding Author

*E-mail: anilkumar@pilani.bits-pilani.ac.in (A.K.).

ORCID

Anil Kumar: 0000-0003-4699-3178

Notes

The authors declare no competing financial interest.

■ ACKNOWLEDGMENTS

The authors sincerely acknowledge financial support [EMR/2016/002242 and PDF/2017/001910] by Science and Engineering Research Board (SERB), New Delhi, to carry out this work, DST-FIST [SR/FST/CSI-270/2015] for HRMS facility and Central Analytical Lab, BITS Pilani, for NMR. N.K.N., S.D., and H.K.S. are grateful to the Council of Scientific and Industrial Research (CSIR), New Delhi, India, for senior research fellowship. The authors also acknowledge Shahid Khan, Department of Biological Science, BITS Pilani, Pilani campus Rajasthan, India for concentration-dependent hemolytic activity.

■ ABBREVIATIONS

MRSA, methicillin-resistant *Staphylococcus aureus*; MIC, minimum inhibitory concentration; ZOI, zone of inhibition; PI, propidium iodide; AO, acridine orange; Et·Br, ethidium bromide; ROS, reactive oxygen species; DCFH-DA, 2′,7′-dichlorofluorescein diacetate; RBC, red blood cell; PBS, phosphate buffer saline; CDC, cross-dehydrogenative coupling; CAN, ceric ammonium nitrate; TBHP, *tert*-butyl hydroperoxide; DMSO, dimethyl sulphoxide; PDB, potato dextrose broth; OD, optical density

■ REFERENCES

(1) Lowy, F. D. Staphylococcus aureus infections. *N. Engl. J. Med.* **1998**, *339*, 520−532.

DOI: 10.1021/acsomega.8b01592
ACS Omega 2018, 3, 16338−16346

(2) Shallcross, L. J.; Davies, S. C. The world health assembly resolution on antimicrobial resistance. *J. Antimicrob. Chemother.* **2014**, *69*, 2883−2885.
(3) (a) Wencewicz, T. A.; Miller, M. J. Biscatecholate−monohydroxamate mixed ligand siderophore−carbacephalosporin conjugates are selective sideromycin antibiotics that target acinetobacter baumannii. *J. Med. Chem.* **2013**, *56*, 4044−4052. (b) Carosso, S.; Liu, R.; Miller, P. A.; Hecker, S. J.; Glinka, T.; Miller, M. J. Methodology for monobactam diversification: Syntheses and studies of 4-thiomethyl substituted β-lactams with activity against gram-negative bacteria, including carbapenemase producing acinetobacter baumannii. *J. Med. Chem.* **2017**, *9*, 8933−8944. (c) Ghosh, M.; Miller, P. A.; Möllmann, U.; Claypool, W. D.; Schroeder, V. A.; Wolter, W. R.; Suckow, M.; Yu, H.; Li, S.; Huang, W.; Zajicek, J.; Miller, M. J. Targeted antibiotic delivery: Selective siderophore conjugation with daptomycin confers potent activity against multidrug resistant acinetobacter baumannii both in vitro and in vivo. *J. Med. Chem.* **2017**, *60*, 4577−4583.
(4) (a) Zhang, H.-Z.; He, S.-C.; Peng, Y.-J.; Zhang, H.-J.; Gopala, L.; Tangadanchu, V. K. R.; Gan, L.-L.; Zhou, C.-H. Design, synthesis and antimicrobial evaluation of novel benzimidazole-incorporated sulfonamide analogues. *Eur. J. Med. Chem.* **2017**, *136*, 165−183. (b) Zhang, W.; Liu, J.; Macho, J. M.; Jiang, X.; Xie, D.; Jiang, F.; Liu, W.; Fu, L. Design, synthesis and antimicrobial evaluation of novel benzoxazole derivatives. *Eur. J. Med. Chem.* **2017**, *126*, 7−14. (c) Ullah, A.; Iftikhar, F.; Arfan, M.; Kazmi, S. T. B.; Anjum, M. N.; Haq, I.-u.; Ayaz, M.; Farooq, S.; Rashid, U. Amino acid conjugated antimicrobial drugs: Synthesis, lipophilicity-activity relationship, antibacterial and urease inhibition activity. *Eur. J. Med. Chem.* **2018**, *145*, 140−153. (d) Sekhar, M. M.; Nagarjuna, U.; Padmavathi, V.; Padmaja, A.; Reddy, N. V.; Vijaya, T. Synthesis and antimicrobial activity of pyrimidinyl 1, 3, 4-oxadiazoles, 1, 3, 4-thiadiazoles and 1, 2, 4-triazoles. *Eur. J. Med. Chem.* **2018**, *145*, 1−10. (e) El-Gohary, N. S.; Shaaban, M. I. Synthesis and biological evaluation of a new series of benzimidazole derivatives as antimicrobial, antiquorum-sensing and antitumor agents. *Eur. J. Med. Chem.* **2017**, *131*, 255−262. (f) Anand, D.; Yadav, P. K.; Patel, O. P. S.; Parmar, N.; Maurya, R. K.; Vishwakarma, P.; Raju, K. S. R.; Taneja, I.; Wahajuddin, M.; Kar, S. Antileishmanial activity of pyrazolopyridine derivatives and their potential as an adjunct therapy with miltefosine. *J. Med. Chem.* **2017**, *60*, 1041−1059.
(5) (a) Hong, W.; Li, J.; Chang, Z.; Tan, X.; Yang, H.; Ouyang, Y.; Yang, Y.; Kaur, S.; Paterson, I. C.; Ngeow, Y. F.; Wang, H. Synthesis and biological evaluation of indole core-based derivatives with potent antibacterial activity against resistant bacterial pathogens. *J. Antibiot.* **2017**, *70*, 832. (b) Lepri, S.; Buonerba, F.; Goracci, L.; Velilla, I.; Ruzziconi, R.; Schindler, B. D.; Seo, S. M.; Kaatz, G. W.; Cruciani, G. Indole based weapons to fight antibiotic resistance: A structure−activity relationship study. *J. Med. Chem.* **2016**, *59*, 867−891. (c) Jafari, E.; Khajouei, M. R.; Hassanzadeh, F.; Hakimelahi, G. H.; Khodarahmi, G. A. Quinazolinone and quinazoline derivatives: Recent structures with potent antimicrobial and cytotoxic activities. *Res. Pharm. Sci.* **2016**, *11*, 1−14.
(6) Hoemann, M. Z.; Kumaravel, G.; Xie, R. L.; Rossi, R. F.; Meyer, S.; Sidhu, A.; Cuny, G. D.; Hauske, J. R. Potent in vitro methicillin-resistant staphylococcus aureus activity of 2-(1H-indol-3-yl) quinoline derivatives. *Bioorg. Med. Chem. Lett.* **2000**, *10*, 2675−2678.
(7) Song, Y.-L.; Wu, F.; Zhang, C.-C.; Liang, G.-C.; Zhou, G.; Yu, J.-J. Ionic liquid catalyzed synthesis of 2-(indole-3-yl)-thiochroman-4-ones and their novel antifungal activities. *Bioorg. Med. Chem. Lett.* **2015**, *25*, 259−261.
(8) Bartik, K.; Braekman, J.-C.; Daloze, D.; Stoller, C.; Huysecom, J.; Vandevyver, G.; Ottinger, R. Topsentins, new toxic bis-indole alkaloids from the marine sponge topsentia genitrix. *Can. J. Chem.* **1987**, *65*, 2118−2121.
(9) Kung, P.-P.; Casper, M. D.; Cook, K. L.; Wilson-Lingardo, L.; Risen, L. M.; Vickers, T. A.; Ranken, R.; Blyn, L. B.; Wyatt, J. R.; Cook, P. D. Structure−activity relationships of novel 2-substituted quinazoline antibacterial agents. *J. Med. Chem.* **1999**, *42*, 4705−4713.
(10) (a) Rohini, R.; Reddy, P. M.; Shanker, K.; Hu, A.; Ravinder, V. Antimicrobial study of newly synthesized 6-substituted indolo[1, 2-c]quinazolines. *Eur. J. Med. Chem.* **2010**, *45*, 1200−1205. (b) Rohini, R.; Shanker, K.; Reddy, P. M.; Ho, Y.-P.; Ravinder, V. Mono and bis-6-arylbenzimidazo[1, 2-c]quinazolines: A new class of antimicrobial agents. *Eur. J. Med. Chem.* **2009**, *44*, 3330−3339. (c) Khan, I.; Zaib, S.; Batool, S.; Abbas, N.; Ashraf, Z.; Iqbal, J.; Saeed, A. Quinazolines and quinazolinones as ubiquitous structural fragments in medicinal chemistry: An update on the development of synthetic methods and pharmacological diversification. *Bioorg. Med. Chem.* **2016**, *24*, 2361−2381. (d) Khan, I.; Ibrar, A.; Ahmed, W.; Saeed, A. Synthetic approaches, functionalization and therapeutic potential of quinazoline and quinazolinone skeletons: The advances continue. *Eur. J. Med. Chem.* **2015**, *90*, 124−169. (e) Khan, I.; Ibrar, A.; Abbas, N.; Saeed, A. Recent advances in the structural library of functionalized quinazoline and quinazolinone scaffolds: Synthetic approaches and multifarious applications. *Eur. J. Med. Chem.* **2014**, *76*, 193−244. (f) Fröhlich, T.; Reiter, C.; Ibrahim, M. M.; Beutel, J.; Hutterer, C.; Zeitträger, I.; Bahsi, H.; Leidenberger, M.; Friedrich, O.; Kappes, B. Synthesis of novel hybrids of quinazoline and artemisinin with high activities against plasmodium falciparum, human cytomegalovirus, and leukemia Cells. *ACS Omega* **2017**, *2*, 2422−2431. (g) Jadhavar, P. S.; Dhameliya, T. M.; Vaja, M. D.; Kumar, D.; Sridevi, J. P.; Yogeeswari, P.; Sriram, D.; Chakraborti, A. K. Synthesis, biological evaluation and structure−activity relationship of 2-styrylquinazolones as anti-tubercular agents. *Bioorg. Med. Chem. Lett.* **2016**, *26*, 2663−2669.
(11) (a) Nandwana, N. K.; Dhiman, S.; Shelke, G. M.; Kumar, A. Copper-catalyzed tandem Ullmann type C-N coupling and dehydrative cyclization: Synthesis of imidazo[1,2-c]quinazolines. *Org. Biomol. Chem.* **2016**, *14*, 1736−1741. (b) Nandwana, N. K.; Dhiman, S.; Saini, H. K.; Kumar, I.; Kumar, A. Synthesis of quinazolinones, imidazo[1, 2-c]quinazolines and imidazo[4, 5-c]quinolines through tandem reductive amination of aryl halides and oxidative amination of C(sp^3)−H bonds. *Eur. J. Org. Chem.* **2017**, 514−522. (c) Kumar, A.; Nandwana, N. K.; Saini, H. K.; Shinde, V. N. Copper-catalysed one-pot tandem reaction for the synthesis of imidazo[1,2-c][1,2,3]-triazolo[1,5-a]quinazolines. *Eur. J. Org. Chem.* **2017**, 6445−6449.
(12) Samai, S.; Nandi, G. C.; Singh, P.; Singh, M. L-Proline: an efficient catalyst for the one-pot synthesis of 2, 4, 5-trisubstituted and 1, 2, 4, 5-tetrasubstituted imidazoles. *Tetrahedron* **2009**, *65*, 10155−10161.
(13) Nandwana, N. K.; Pericherla, K.; Kaswan, P.; Kumar, A. Synthesis of novel azole-fused quinazolines via one-pot, sequential Ullmann-type coupling and intramolecular dehydrogenative C−N bonding. *Org. Biomol. Chem.* **2015**, *13*, 2947−2950.
(14) Tyagi, P.; Singh, M.; Kumari, H.; Kumari, A.; Mukhopadhyay, K. Bactericidal activity of curcumin I is associated with damaging of bacterial membrane. *PLoS One* **2015**, *10*, No. e0121313.
(15) Stiefel, P.; Schmidt-Emrich, S.; Maniura-Weber, K.; Ren, Q. Critical aspects of using bacterial cell viability assays with the fluorophores SYTO9 and propidium iodide. *BMC Microbiol.* **2015**, *15*, 36.
(16) (a) Kasibhatla, S.; Amarante-Mendes, G. P.; Finucane, D.; Brunner, T.; Bossy-Wetzel, E.; Green, D. R. Acridine orange/ethidium bromide (AO/EB) staining to detect apoptosis. *Cold Spring Harb. Protoc.* **2006**, *3*, prot4493. (b) Ribble, D.; Goldstein, N. B.; Norris, D. A.; Shellman, Y. G. A simple technique for quantifying apoptosis in 96-well plates. *BMC Biotechnol.* **2005**, *5*, 12.
(17) Simpson, E. H. *Prevalence of Penicillin-Resistant Streptococcus Pneumoniae-Connecticut, 1992−1993*; Library Publications and Presentations, 1994; Vol. *43*.
(18) Sathishkumar, G.; Jha, P. K.; Vignesh, V.; Rajkuberan, C.; Jeyaraj, M.; Selvakumar, M.; Jha, R.; Sivaramakrishnan, S. Cannonball fruit (Couroupita guianensis, Aubl.) extract mediated synthesis of gold nanoparticles and evaluation of its antioxidant activity. *J. Mol. Liq.* **2016**, *215*, 229−236.

DOI: 10.1021/acsomega.8b01592
ACS Omega 2018, 3, 16338−16346